Vortex in a trapped Bose-Einstein condensate with dipole-dipole interactions

D. H. J. O'Dell[1] and C. Eberlein[2]
[1]*Centre for Cold Matter, The Blackett Laboratory, Imperial College, London SW7 2BW, United Kingdom*
[2]*Department of Physics & Astronomy, University of Sussex, Falmer, Brighton BN1 9QH, United Kingdom*
(Received 14 August 2006; published 4 January 2007)

We calculate the critical rotation frequency at which a vortex state becomes energetically favorable over the vortex-free ground state in a harmonically trapped Bose-Einstein condensate whose atoms have dipole-dipole interactions as well as the usual *s*-wave contact interactions. In the Thomas-Fermi (hydrodynamic) regime, dipolar condensates in oblate cylindrical traps (with the dipoles aligned along the axis of symmetry of the trap) tend to have lower critical rotation frequencies than their purely *s*-wave contact interaction counterparts. The converse is true for dipolar condensates in prolate traps. Quadrupole excitations and center of mass motion are also briefly discussed as possible competing mechanisms to a vortex as means by which superfluids with partially attractive interactions might carry angular momentum.

DOI: 10.1103/PhysRevA.75.013604 PACS number(s): 03.75.Lm, 34.20.Cf, 32.10.Dk, 75.80.+q

I. INTRODUCTION

The achievement of Bose-Einstein condensation in a trapped gas of ^{52}Cr atoms by the Stuttgart group [1] is the first instance of a condensate with large dipole-dipole interactions. In comparison to alkali atoms, which have a maximum magnetic dipole moment of $\mu=1\mu_B$ (μ_B is the Bohr magneton), chromium atoms possess an anomalously large magnetic dipole moment of $\mu=6\mu_B$. The long-range part of the interaction between two dipoles separated by $\mathbf{r}$, and aligned by an external field along a unit vector $\hat{\mathbf{e}}$ (in this paper we shall always assume the dipoles are aligned by an external field), is given by

$$U_{\rm dd}(\mathbf{r}) = \sum_{i,j} \frac{C_{\rm dd}}{4\pi} \hat{e}_i \hat{e}_j \frac{(\delta_{ij} - 3\hat{r}_i \hat{r}_j)}{r^3}, \tag{1}$$

where the coupling $C_{\rm dd}=\mu_0\mu^2$ depends on the square of the dipole moment. Chromium atoms also have shorter range isotropic interactions which are asymptotically of the van der Waals-type and so fall off as r^{-6}. At ultralow temperatures the de Broglie wavelength of the atoms is much larger than the range of the isotropic interactions which can consequently be handled within perturbation theory by using the usual delta-function pseudopotential [2]

$$U(\mathbf{r}) = 4\pi\hbar^2 a_{\rm s} \delta(\mathbf{r})/m \equiv g\,\delta(\mathbf{r}) \tag{2}$$

characterized solely by the *s*-wave scattering length a_s. A measure of the strength of the long-range dipole-dipole interaction relative to the *s*-wave scattering energy is given by the dimensionless quantity

$$\varepsilon_{\rm dd} \equiv \frac{C_{\rm dd}}{3g}. \tag{3}$$

For ^{87}Rb one finds $\varepsilon_{\rm dd}\approx 0.007$, and Na has $\varepsilon_{\rm dd}\approx 0.004$. Taking the *s*-wave scattering length of ^{52}Cr to be $a_s=105a_{\rm B}$ [1], one obtains $\varepsilon_{\rm dd}\approx 0.144$. In a further significant development, the Stuttgart group has also studied Feshbach scattering resonances between ^{52}Cr atoms [3]. This means that the magnitude and sign of a_s, and thus also the value of $\varepsilon_{\rm dd}$, can be controlled.

The principal effect of the anisotropy of the dipole-dipole interactions upon a stationary, trapped condensate will be to distort its aspect ratio so that it is elongated along the direction of the external field [4,5]. This is in contrast to the case of purely isotropic interactions, for which the aspect ratio of the condensate matches that of the trap. By adopting an elongated aspect ratio along the direction of polarization, the condensate achieves a lower energy by placing more dipoles end-to-end, in which configuration they are attractive, and reducing the number of repulsive side-by-side interactions. When $\varepsilon_{\rm dd}$ exceeds a certain value, which in general depends on the aspect ratio of the trap as well as the total number of atoms *N*, mean-field theory predicts that the condensate becomes unstable to collapse [4–8]. The partially attractive nature of the dipole-dipole interaction is also responsible for introducing a curious "roton" minimum [9,10] into the Bogoliubov excitation spectrum of a uniform dipolar Bose-Einstein condensate (BEC), reminiscent of that found in the excitation spectrum of liquid helium II. It is possible that this roton minimum is indicative of an instability towards the formation of a density wave [11,12].

The fact that the interaction between dipoles aligned by an external field along the axis of symmetry of a cylindrical trap are on average repulsive in an oblate (pancake shaped) BEC, but, conversely, are on average attractive in a prolate (cigar shaped) BEC, means that the sign of the dipolar mean-field energy can be controlled via the aspect ratio of the trap. In this paper we are interested in calculating the effect that this change of aspect ratio of the trap has upon the vortex state in a rotating dipolar BEC. The case of a vortex in a rotating BEC with repulsive short-range interactions, as described by Eq. (2) with $a_s>0$, has been extensively studied both theoretically, e.g., [13–15], and experimentally, e.g., [16–18]. Attractive short-range interactions have, on the other hand, received comparatively less attention, although a rotating BEC with attractive interactions is of considerable fundamental interest [19]. In particular, when the interactions are attractive it is intuitively plausible that vortex formation will be suppressed because it is energetically expensive to form the vortex core since this requires moving atoms from the center of the BEC where they interact with many other atoms and placing them on the edges where they interact

with fewer [20]. Instead, it has been proposed that the angular momentum might be preferentially absorbed into other types of excitation, such as center of mass motion or shape oscillations, which cause much less disturbance to the condensate density profile and internal correlations [19,21]. We also note that a recent theoretical study of a two-dimensional BEC with purely attractive short-range interactions found a new class of vortices in the form of bright ring solitons [22]. When it comes to dipolar interactions, which are partly attractive, partly repulsive, one might therefore anticipate rotational properties similar to those of standard BECs with either attractive or repulsive interactions, depending upon whether the dipolar BEC is prolate or oblate, respectively.

The latest experiments on chromium [23] have detected the first evidence of dipolar interactions upon the dynamics of a BEC by observing the ballistic expansion of the BEC when the trap is switched off. The results are in good agreement with theoretical predictions [24] giving us some confidence in the theory of dipolar BECs which has been built up over the last six years. In the following we will discuss a vortex in a rotating dipolar BEC in the Thomas-Fermi (hydrodynamic) regime, which is defined as being when the quantum zero-point kinetic energy due to the confinement by the trap is negligible in comparison to the trapping and interaction energies. This is the relevant regime when there are a large number of atoms. We shall make extensive use of the exact results for dipolar BECs in the Thomas-Fermi limit reported in Refs. [25,26]. The key insight of those papers was that the dipolar mean-field potential that the atomic dipoles feel, and which is nonlocal, i.e., depends on the entire atom distribution, can be expressed in terms of derivatives of a scalar potential that is a solution of the Poisson equation with the dipolar density as a source. In other words, this scalar potential is formally equivalent to the electrostatic potential one would get if the density distribution were not one of dipoles but of charges, and thus standard mathematical techniques known from electrostatics can be applied. Three recent theory papers [27–29] have dealt with the structure of vortex lattices in dipolar BECs, but our aim here is to investigate the differences between dipolar and nondipolar condensates in the case of a single vortex. Our main concern will be the calculation of the critical rotation frequency Ω_c necessary to make a single vortex energetically favorable over the ground state. Note that Ref. [29] also deals with the single vortex case, but their focus was somewhat different. One of their principle results was that in the case of dipolar interactions plus *attractive* contact interactions (negative scattering length) the vortices develop a "craterlike" structure which is probably connected with the density wave instability mentioned above. We shall not explicitly consider negative scattering lengths here because we wish to use some exact results that only hold in the Thomas-Fermi limit. A dipolar BEC with attractive short-range interactions is unstable to collapse in the Thomas-Fermi limit and so we limit ourselves to $a_s > 0$.

II. ENERGY FUNCTIONAL FOR A DIPOLAR BEC WITH A VORTEX

Consider a condensate at $T=0$ with a wave function $\Psi(\mathbf{r})$ normalized to the total number of atoms $\int|\Psi(\mathbf{r})|^2 d^3r = N$. The general form of $\Psi(\mathbf{r})$ when there is one singly quantized vortex present can be expressed in cylindrical coordinates (ρ, ϕ, z) as $\Psi(\mathbf{r}) = |\Psi(\rho, z)|\exp(i\phi)$ [2]. This state carries an angular momentum $L_z = N\hbar$. In a frame rotating at angular velocity Ω about the z-axis the energy of the condensate becomes $E' = E - \Omega L_z$, where the angular momentum L_z and energy E are those pertaining to the laboratory frame. However, creating a vortex costs energy. Denoting the energy of the BEC in its ground state without any vortex ($L_z=0$) by E_0 and the extra energy needed to make a single vortex by E_v, we can write the energy of the vortex state in the rotating frame as

$$E' = E_0 + E_v - \Omega L_z. \tag{4}$$

Thus we see that for a BEC at equilibrium in a trap rotating at angular velocity Ω the vortex state becomes energetically favorable when Ω exceeds a critical rotational velocity

$$\Omega_c = \frac{E_v}{N\hbar}. \tag{5}$$

To obtain Ω_c we thus need to evaluate the extra energy associated with the formation of the vortex. The total energy functional for a trapped dipolar BEC can be written as

$$E_{\text{tot}} = E_{\text{kinetic}} + E_{\text{trap}} + E_{\text{sw}} + E_{\text{dd}}, \tag{6}$$

where, in terms of the condensate wave function $\Psi(\mathbf{r})$,

$$E_{\text{kinetic}} = -\frac{\hbar^2}{2m}\int d^3r\, \Psi^*(\mathbf{r})\nabla^2\Psi(\mathbf{r}) \tag{7}$$

is the kinetic energy, and

$$E_{\text{trap}} = \frac{m}{2}\omega_x^2 \int d^3r\, |\Psi(\mathbf{r})|^2[\rho^2 + \gamma^2 z^2] \tag{8}$$

is the energy due to the harmonic trap $V_{\text{trap}} = (m/2)\omega_x^2[\rho^2 + \gamma^2 z^2]$, where $\rho^2 = x^2 + y^2$ and

$$\gamma \equiv \omega_z/\omega_x \tag{9}$$

is the ratio of the trap frequencies. Note that in this paper we shall assume that both the trap and the condensate are cylindrically symmetric about the $\hat{z}$ direction, so in particular $\omega_x = \omega_y$, and the external field responsible for aligning the dipoles is along the $\hat{z}$ axis.

The total mean-field interaction energy can to a good approximation [5] be written as the sum of two parts. The first is due to the isotropic short-range interactions which give rise to pure s-wave scattering

$$E_{\text{sw}} = \frac{g}{2}\int d^3r|\Psi(\mathbf{r})|^4 \tag{10}$$

and the second is due to dipole-dipole interactions

$$E_{\text{dd}} = \frac{1}{2}\int d^3r\, d^3r'\, |\Psi(\mathbf{r})|^2 U_{\text{dd}}(\mathbf{r}-\mathbf{r}')|\Psi(\mathbf{r}')|^2. \tag{11}$$

The long-range and anisotropic nature of the dipole-dipole interaction, $U_{\text{dd}}(\mathbf{r})$, makes the calculation of E_{dd} a nontrivial exercise. However, in the Thomas-Fermi regime some exact

results (within mean-field theory) are available. In particular, an exact solution of the vortex-free Thomas-Fermi problem for a dipolar BEC in a harmonic trap yields a density profile which is an inverted parabola [25,26]. This solution is similar to the familiar nondipolar case [2], except that the aspect ratio of the cloud in the dipolar case is no longer identical to that of the trap but is stretched along the direction of the polarizing field, as mentioned above. By applying scaling transformations to this exact solution one can also describe the lowest energy collective excitations of the condensate [25], as well as the expansion dynamics when the trap is turned off. In the Thomas-Fermi regime the critical ratio of the dipolar and *s*-wave interactions above which instabilities occur is $\varepsilon_{\rm dd}=1$ [30]. The occurrence of these instabilities is indicated by the appearance of imaginary frequencies for the collective excitations. Another particularly novel instability in a trapped dipolar BEC, which originates from the long-range nature of the interatomic interactions, is the appearance of a local minimum in the mean-field potential *outside* the condensate when $\varepsilon_{\rm dd}>1$. This stimulates the formation of a "Saturn-ring" around the condensate as atoms tunnel into the minimum [26].

As explained at length in Refs. [25,26], the dipole-dipole interaction can be reexpressed so as to take advantage of the large technical machinery that exists to deal with electrostatic interactions. In general one can write

$$E_{\rm dd}=\frac{1}{2}\int d^3r n(\mathbf{r})\Phi_{\rm dd}(\mathbf{r}) \tag{12}$$

where $\Phi_{\rm dd}(\mathbf{r})$ is the nonlocal dipolar mean-field potential

$$\Phi_{\rm dd}(\mathbf{r})\equiv\int d^3r' U_{\rm dd}(\mathbf{r}-\mathbf{r}')n(\mathbf{r}'). \tag{13}$$

For dipoles aligned along $\hat{z}$ this dipolar mean-field potential can in turn be expressed in terms of a fictitious electrostatic potential $\phi(\mathbf{r})$

$$\Phi_{\rm dd}(\mathbf{r})=-C_{\rm dd}\left(\frac{\partial^2}{\partial z^2}\phi(\mathbf{r})+\frac{n(\mathbf{r})}{3}\right), \tag{14}$$

which is obtained from the "charge" distribution $n(\mathbf{r})$ in the usual way

$$\phi(\mathbf{r})=\frac{1}{4\pi}\int d^3r'\frac{n(\mathbf{r}')}{|\mathbf{r}-\mathbf{r}'|}, \tag{15}$$

where, of course, $n(\mathbf{r})$ and $\phi(\mathbf{r})$ satisfy Poisson's equation $\nabla^2\phi=-n(\mathbf{r})$. This formulation of the problem allows us to immediately identify some generic features of dipolar gases. For example, if $n(\mathbf{r})$ and hence $\phi(\mathbf{r})$ are uniform along the polarization direction ($\hat{z}$) then the nonlocal part of the dipolar interaction vanishes because of the $\partial^2/\partial z^2$ operator. A very prolate (pencil-like) condensate, i.e., one which has $R_z\gg R_x,R_y$ will therefore be largely unaffected by the nonlocal part of the interaction (except at the very ends of the condensate where the density profile has a large curvature). Thus in the very prolate (or entirely homogenous) case the contribution of dipolar interactions to the mean-field potential reduces to that of the local term $\Phi_{\rm dd}(\mathbf{r})\to-C_{\rm dd}n(\mathbf{r})/3$ whose effect is then simply to modify the magnitude of the local mean-field potential arising from the pure *s*-wave interactions. With these considerations in mind, we note that the effect of a vortex upon $\Phi_{\rm dd}$ is likely to be greatest when the vortex axis lies in the $x-y$ plane so that the rapid density variation due to the vortex core lies in the z direction. However, because of lack of symmetry, we shall not consider this situation further here.

Let us consider the case of a parabolic density profile of the form

$$n_{\rm bg}(\mathbf{r})=n_0\left(1-\frac{\rho^2}{R_x^2}-\frac{z^2}{R_z^2}\right). \tag{16}$$

As stated above, a parabolic density profile is an exact solution of the hydrodynamic equations for a nonrotating BEC in the Thomas-Fermi limit even in the presence of dipolar interactions. Here the subscript "bg" stands for "background," i.e., for a condensate without a vortex but on top of which we will superimpose a vortex later on. One finds that the dipolar mean-field potential inside a condensate with the parabolic density profile (16) is given by [25,26]

$$\Phi_{\rm dd}^{\rm bg}(\rho,z)=\frac{n_0C_{\rm dd}}{3}\left[\frac{\rho^2}{R_x^2}-\frac{2z^2}{R_z^2}-f(\kappa)\left(1-\frac{3}{2}\frac{\rho^2-2z^2}{R_x^2-R_z^2}\right)\right]. \tag{17}$$

In this expression

$$f(\kappa)\equiv\frac{2+\kappa^2[4-3\Xi(\kappa)]}{2(1-\kappa^2)} \tag{18}$$

is a function of κ which is the aspect ratio of the BEC,

$$\kappa\equiv R_x/R_z \tag{19}$$

and monotonically decreases from its value of $f=1$ at $\kappa=0$, passing through zero at $\kappa=1$, tending towards $f=-2$ as $\kappa\to\infty$. The function $\Xi(\kappa)$ upon which $f(\kappa)$ depends is itself dependent upon whether the condensate density profile is prolate, in which case

$$\Xi\equiv\frac{1}{\sqrt{1-\kappa^2}}\ln\frac{1+\sqrt{1-\kappa^2}}{1-\sqrt{1-\kappa^2}}\quad\text{for }\kappa<1\text{ (prolate)} \tag{20}$$

or oblate

$$\Xi\equiv\frac{2}{\sqrt{\kappa^2-1}}\arctan\sqrt{\kappa^2-1}\text{ for }\kappa>1\text{ (oblate)}. \tag{21}$$

The value of the aspect ratio κ is given by the solution of a transcendental equation [5,24–26]

$$3\kappa^2\varepsilon_{\rm dd}\left[\left(\frac{\gamma^2}{2}+1\right)\frac{f(\kappa)}{1-\kappa^2}-1\right]+(\varepsilon_{\rm dd}-1)(\kappa^2-\gamma^2)=0. \tag{22}$$

Note that according to Eq. (17), the dipolar mean-field potential $\Phi_{\rm dd}^{\rm bg}(\rho,z)$ is in general saddle-shaped [23], and thus inherits the anisotropic partially attractive/partially repulsive character of the dipolar interactions. The saddle shaped mean-field potential causes an elongation of the BEC along

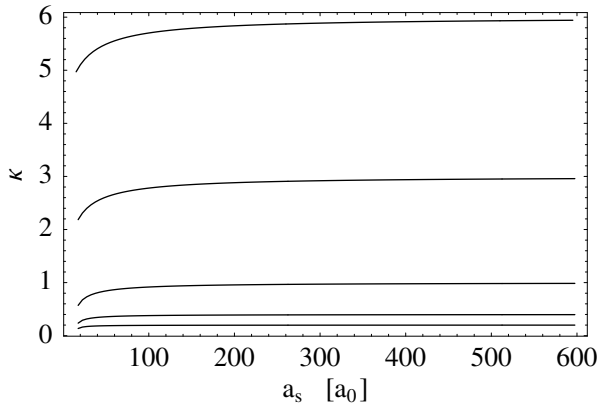

FIG. 1. Aspect ratio $\kappa=R_x/R_z$ of a vortex-free dipolar BEC as a function of scattering length a_s (measured in units of the Bohr radius a_0) in the Thomas-Fermi limit. In descending order, the curves are for traps with aspect ratios $\gamma=\omega_z/\omega_x=6$, 3, 1, 0.4, and 0.2. When $a_s\to\infty$ the s-wave contact interactions dominate and the aspect ratio matches that of the trap, i.e., $\kappa=\gamma$, given by the right-hand asymptote of each curve. When $a_s\to 0$ the dipolar interactions dominate and their magnetostrictive effect reduces κ below the pure s-wave value. In the limit $a_s\to 0$ a dipolar BEC will collapse towards a chain of end-to-end dipoles and mean-field theory will breakdown. In this figure $C_{\rm dd}=\mu_0(6\mu_{\rm B})^2$ and the minimum value of scattering length shown is $a_s=17.5a_0$.

the polarization direction which can be viewed as a type of magnetostriction. This is illustrated for five different trap aspect ratios in Fig. 1. The total energy $(E_{\rm trap}+E_{\rm sw}+E_{\rm dd})$ associated with the vortex-free Thomas-Fermi solution (16) can be calculated to be [26]

$$E_0=\frac{N}{14}m\omega_x^2R_x^2\left(2+\frac{\gamma^2}{\kappa^2}\right)+\frac{15}{28\pi}\frac{N^2g}{R_x^2R_z}[1-\varepsilon_{\rm dd}f(\kappa)]. \quad (23)$$

The quantity E_0 is the ground state energy referred to in Eq. (4).

Having now summarized what is already known concerning the mean-field potential inside a nonrotating dipolar BEC, let us turn to the form of the density profile of a rotating BEC with a vortex. We shall adopt the following variational ansatz for the density profile of an N-atom condensate with a single vortex:

$$n(\mathbf{r})\equiv|\Psi(\mathbf{r})|^2=n_0\left(1-\frac{\rho^2}{R_x^2}-\frac{z^2}{R_z^2}\right)\left(1-\frac{\beta^2}{\rho^2+\beta^2}\right) \quad (24)$$

$$=n_{\rm bg}(\mathbf{r})+n_{\rm v}(\mathbf{r}), \quad (25)$$

where we have observed that the ansatz can be written as the sum of two terms: the background Thomas-Fermi parabolic profile $n_{\rm bg}(\mathbf{r})$ as already given in Eq. (16) and the vortex profile $n_{\rm v}(\mathbf{r})$

$$n_{\rm v}(\mathbf{r})=-n_0\frac{\beta^2}{\rho^2+\beta^2}\left(1-\frac{\rho^2}{R_x^2}-\frac{z^2}{R_z^2}\right). \quad (26)$$

Ansatz (24) assumes that the vortex, whose core size is parametrized by β, is superimposed on a background parabolic density profile with radii $R_x=R_y$ and R_z. Note that the variational ansatz (24) has the correct $\rho^{2\ell}$ dependence of the density as $\rho\to 0$ (with $\ell=1$), which it must have in order to satisfy the Gross-Pitaevskii equation for a vortex of ℓ circulation quanta [21]. It has also got the correct asymptotic form (in terms of even powers of $1/\rho$) that the solution must have for $\rho\to\infty$. The central density n_0 is fixed by normalization to be

$$n_0=\frac{15N}{8\pi R_x^2R_z}\Bigg/\left(1+\frac{20}{3}\bar{\beta}^2+5\bar{\beta}^4-5\bar{\beta}^2(1+\bar{\beta}^2)^{3/2}\,\mathrm{arctanh}[1/\sqrt{1+\bar{\beta}^2}]\right), \quad (27)$$

where

$$\bar{\beta}\equiv\beta/R_x \quad (28)$$

is the ratio of the vortex core size to the transverse radius of the BEC.

We proceed by minimizing $E_{\rm tot}$ as a function of the three variational parameters R_x, R_z, and β. The terms $E_{\rm kinetic}$, $E_{\rm trap}$, and $E_{\rm sw}$ can all be calculated analytically in a straightforward albeit laborious manner. The results are presented in the Appendix. To evaluate the dipole-dipole energy functional we begin from Eq. (11) and substitute in the density ansatz (25)

$$\begin{aligned}E_{\rm dd}=&\frac{1}{2}\int d^3r\,d^3r'\,n_{\rm bg}(\mathbf{r})U_{\rm dd}(\mathbf{r}-\mathbf{r}')n_{\rm bg}(\mathbf{r}')\\&+\frac{1}{2}\int d^3r\,d^3r'\,n_{\rm bg}(\mathbf{r})U_{\rm dd}(\mathbf{r}-\mathbf{r}')n_{\rm v}(\mathbf{r}')\\&+\frac{1}{2}\int d^3r\,d^3r'\,n_{\rm v}(\mathbf{r})U_{\rm dd}(\mathbf{r}-\mathbf{r}')n_{\rm bg}(\mathbf{r}')\\&+\frac{1}{2}\int d^3r\,d^3r'\,n_{\rm v}(\mathbf{r})U_{\rm dd}(\mathbf{r}-\mathbf{r}')n_{\rm v}(\mathbf{r}').\end{aligned}$$

Noting that the two cross terms between the vortex and background densities are identical, i.e., the integral is invariant under exchange of the coordinates $\mathbf{r}$ and $\mathbf{r}'$, we write the dipolar energy functional as

$$\begin{aligned}E_{\rm dd}=&\frac{1}{2}\int d^3r\,d^3r'\,n_{\rm bg}(\mathbf{r})U_{\rm dd}(\mathbf{r}-\mathbf{r}')n_{\rm bg}(\mathbf{r}')\\&+\int d^3r\,d^3r'\,n_{\rm v}(\mathbf{r})U_{\rm dd}(\mathbf{r}-\mathbf{r}')n_{\rm bg}(\mathbf{r}')\\&+\frac{1}{2}\int d^3r\,d^3r'\,n_{\rm v}(\mathbf{r})U_{\rm dd}(\mathbf{r}-\mathbf{r}')n_{\rm v}(\mathbf{r}').\end{aligned}$$

We shall now restrict ourselves to situations where the size of the vortex core is much smaller than the radius of the condensate, i.e., $\bar{\beta}\ll 1$. This is consistent with the spirit of the Thomas-Fermi approximation for the background parabolic envelope, and should hold for condensates containing a large number of atoms, providing the system does not become very prolate. To this end we shall drop the vortex-vortex part of the dipolar energy functional since this has an

extra factor of $\bar{\beta}^2$ in comparison to the cross term. The remaining two terms can be expressed as

$$E_{\rm dd} \approx \frac{1}{2}\int d^3r\, d^3r' n_{\rm bg}(\mathbf{r}) U_{\rm dd}(\mathbf{r}-\mathbf{r}') n_{\rm bg}(\mathbf{r}') + \int d^3r\, d^3r' n_{\rm v}(\mathbf{r}) U_{\rm dd}(\mathbf{r}-\mathbf{r}') n_{\rm bg}(\mathbf{r}') = \frac{1}{2}\int d^3r\, n_{\rm bg}(\mathbf{r})\Phi_{\rm dd}^{\rm bg}(\mathbf{r}) + \int d^3r\, n_{\rm v}(\mathbf{r})\Phi_{\rm dd}^{\rm bg}(\mathbf{r}). \quad (29)$$

The first term is just the dipolar energy of the condensate without a vortex, while the second gives the dipolar "interaction" between the vortex and the background density profile. Both terms have been reduced to single integrals of their respective density profiles over the known quadratic function $\Phi_{\rm dd}^{\rm bg}(\rho,z)$, as given by Eq. (17), which is the mean-field potential due to the background inverted parabola density profile. These integrals can therefore be evaluated relatively easily and the results are given in the Appendix.

III. RESULTS OF MINIMIZATION OF THE ENERGY FUNCTIONAL

A. Oblate trap

To illustrate the oblate case we shall consider 150 000 ^{52}Cr atoms in a trap having frequencies $\omega_x=\omega_y=2\pi\times 200$ rad/s, $\omega_z=2\pi\times 1000$ rad/s, so that $\gamma=5$. The harmonic oscillator length of the trap along the x-direction is then $a_{\rm ho}=\sqrt{\hbar/m\omega_x}=0.986$ μm. We numerically minimize the total energy functional $E_{\rm tot}$ with respect to $\{\beta,R_x,\kappa\}$ using the MATHEMATICA routine *NMinimize*. In order to bring out the dependence of the various quantities upon the relative strength of the two types of interactions (s-wave and dipolar) we plot the results as a function of the s-wave scattering length a_s, since this quantity can be controlled in an experiment [3]. As $a_s\to 0$ the dipolar interactions dominate, whereas when $a_s\to\infty$ the dipolar interactions become insignificant (cf. Fig. 1). The magnitude of the magnetic dipole interaction is here assumed to be fixed at the appropriate value for ^{52}Cr, namely $C_{\rm dd}=\mu_0(6\mu_B)^2$. Note that in the case of dipoles induced by electric fields one has $C_{\rm dd}=E^2\alpha^2/\epsilon_0$ [31], where α is the polarizability and E is the electric field strength, so the size of the electric dipolar interaction can be directly controlled via the magnitude of E. In fact the magnitude of even magnetic dipolar interactions can be controlled independently of the s-wave interactions by rotating the magnetic field [32], but we presume that the experimentally easiest option is to use a Feshbach resonance to adjust a_s since only the magnitude of the magnetic field needs to be tuned.

In all the calculations depicted in the following figures we have limited the minimum value of the scattering length to be $17.5a_0$, where a_0 is the Bohr radius, corresponding to $\varepsilon_{\rm dd}=0.87$. This is because as $a_s\to 0$ the approximation we made in the calculation of the energy functional that $\bar{\beta}=\beta/R_x$ be small begins to breakdown (see Figs. 4 and 9). Furthermore, in the Thomas-Fermi approximation used here collapse instabilities can occur when $\varepsilon_{\rm dd}>1$. Indeed, as mentioned previously, because of these collapse instabilities one can argue that the Thomas-Fermi regime does not exist when $\varepsilon_{\rm dd}>1$, see [26]. The maximum value of scattering length was set at $600a_0$, corresponding to $\varepsilon_{\rm dd}=0.03$.

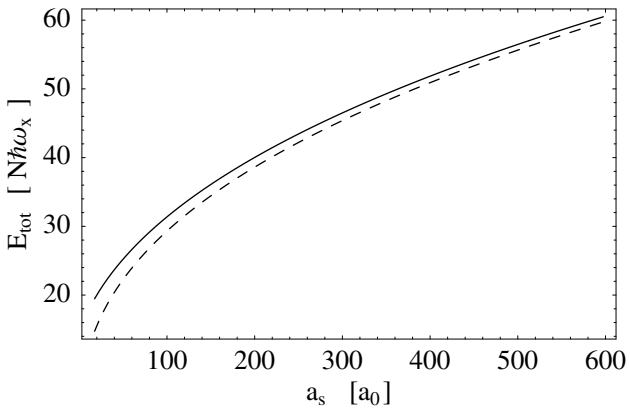

FIG. 2. Total energy (in the Thomas-Fermi approximation) of a dipolar BEC with a vortex in an oblate trap ($\gamma=5$). Solid curve: both s-wave and dipolar interactions. Dashed curve: s-wave only. The s-wave scattering length a_s is measured in units of the Bohr radius a_0. The energy $E_{\rm tot}$ is measured in units of the radial harmonic trapping energy of N atoms.

Figure 2 shows the total energy $E_{\rm tot}$, as defined by Eq. (6), of a condensate with a vortex in an oblate trap. In an oblate BEC the dipolar interactions are predominantly repulsive, which raises the energy relative to the s-wave only case.

Figure 3 plots the radial size R_x of a condensate with a vortex. In a strongly oblate BEC such as this one the majority of atoms interact via the radially repulsive part of the dipolar interaction which consequently increases R_x slightly above the pure s-wave value.

Figure 4 shows $\bar{\beta}=\beta/R_x$, the ratio of the vortex core size to the radial size of the condensate. Note that this ratio remains small over the chosen range of parameters, which, as mentioned above, is necessary for the self-consistency of the calculation. In an oblate trap we see that the effect of the

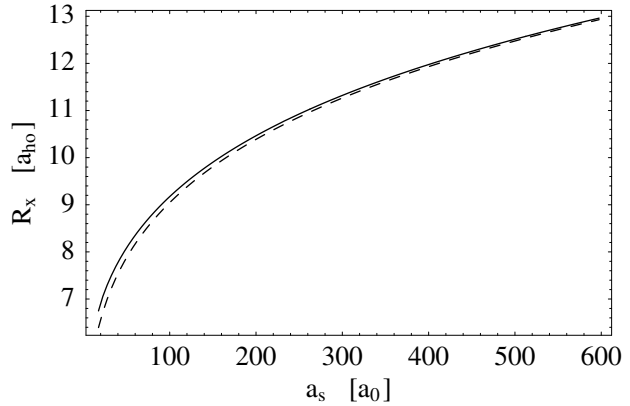

FIG. 3. The radial size R_x of a condensate with a vortex in an oblate trap ($\gamma=5$). Solid curve: both s-wave and dipolar interactions. Dashed curve: s-wave only. R_x is measured in units of the radial harmonic oscillator length $a_{\rm ho}$ of the trap.

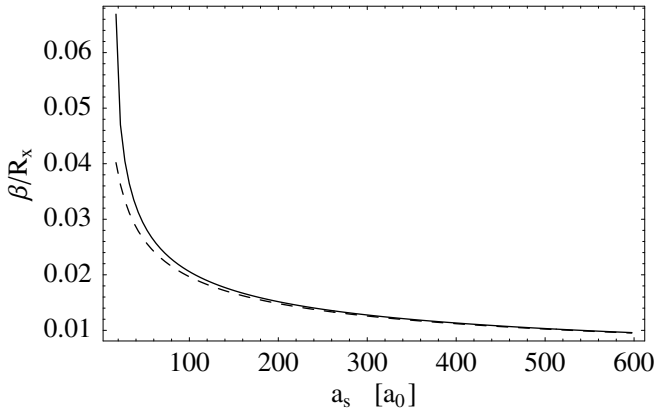

FIG. 4. The ratio of the vortex core size β to the radial size R_x of a condensate in an oblate trap (γ=5). Solid curve: both *s*-wave and dipolar interactions. Dashed curve: *s*-wave only.

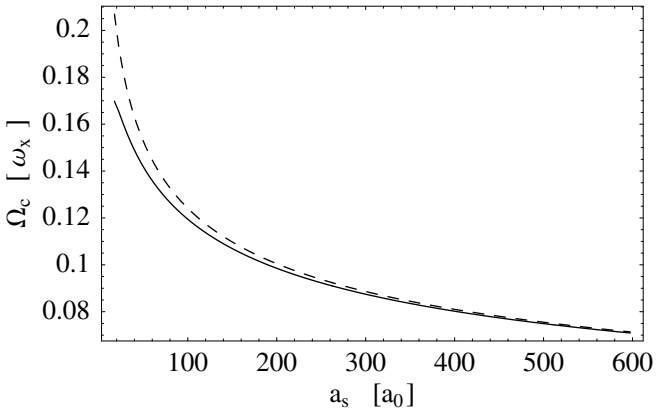

FIG. 6. The critical angular velocity Ω_c above which a vortex state is energetically favorable in an oblate trap (γ=5). Solid curve: both *s*-wave and dipolar interactions. Dashed curve: *s*-wave only. These curves were calculated using Eq. (5). Ω_c is measured in units of the radial harmonic oscillator angular frequency ω_x of the trap.

dipolar interactions is to increase $\bar{\beta}$ beyond that found in the pure *s*-wave case.

Figure 5 depicts the aspect ratio $\kappa=R_x/R_z$ of a condensate with a vortex. The magnetostriction that reduces κ by elongating the condensate is clearly visible.

Figure 6 gives the critical angular velocity Ω_c of the condensate above which it is energetically favorable to form a vortex. We see that the effect of dipolar interactions in an oblate trap is to *decrease* Ω_c.

B. Prolate trap

We now turn to the case of a prolate trap for which the dipolar interactions are predominantly attractive. We choose a trap which has the inverse aspect ratio to the previous oblate case, namely with frequencies $\omega_x=\omega_y=2\pi\times 200$ rad/s as before, so that the harmonic oscillator length of the trap along the *x*-direction remains the same, but with $\omega_z=2\pi\times 40$ rad/s, so that γ=0.2.

Figure 7 depicts the total energy E_{tot} of the vortex state in a prolate trap. The effect of the mainly attractive dipolar interactions is to shift the energy downwards, oppositely to the case of an oblate trap.

Figure 8 plots the radial size, R_x, of a dipolar condensate with a vortex in a prolate trap. R_x is smaller than in the pure *s*-wave case because of the redistribution of atoms by the anisotropic interactions.

Figure 9 shows the ratio of the vortex core size to the radial size of the condensate, $\bar{\beta}=\beta/R_x$. Note that this ratio remains small over the chosen range of parameters, which is necessary for the self-consistency of the calculation, although not as small as in the oblate case. Notice also that in comparison the pure *s*-wave case $\bar{\beta}$ is smaller in the presence of dipolar interactions in a prolate trap, and this trend is opposite to that found in an oblate trap.

Figure 10 gives the aspect ratio $\kappa=R_x/R_z$ of a condensate with a vortex in a prolate trap. Due to the magnetostriction κ is smaller than in the pure *s*-wave case. This is the same behavior as was found in an oblate trap.

Figure 11 shows that, in contrast to the oblate case, the dipolar interactions in a prolate trap *increase* the value of the critical angular velocity Ω_c of the condensate above which it is energetically favorable to form a vortex.

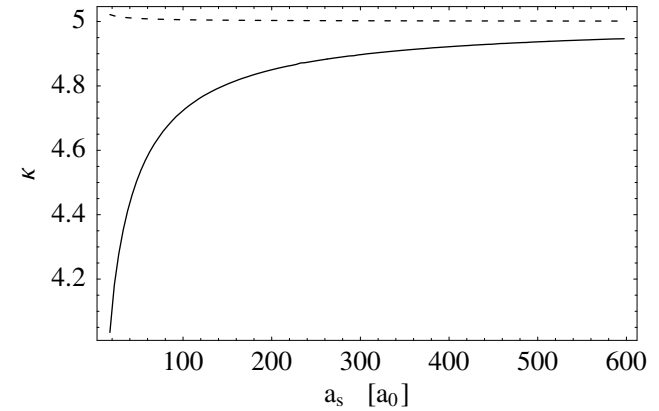

FIG. 5. The aspect ratio κ of a condensate with a vortex in an oblate trap (γ=5). Solid curve: both *s*-wave and dipolar interactions. Dashed curve: *s*-wave only.

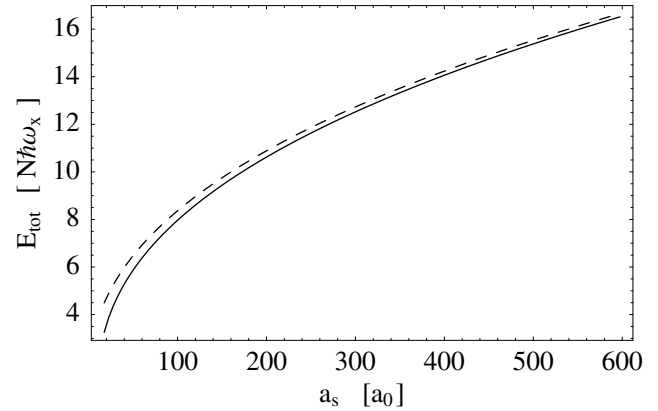

FIG. 7. Total energy (in the Thomas-Fermi approximation) of a dipolar BEC with a vortex in a prolate trap (γ=0.2). Solid curve: both *s*-wave and dipolar interactions. Dashed curve: *s*-wave only.

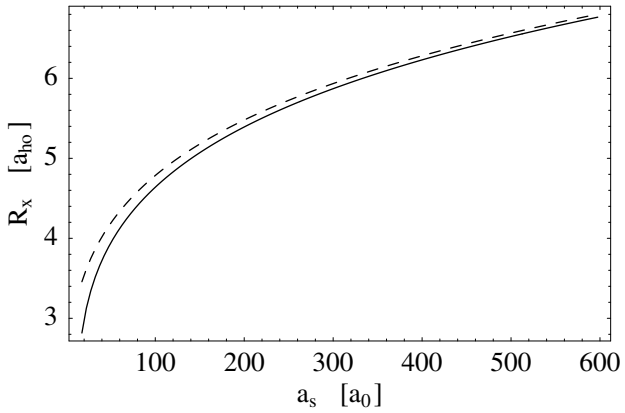

FIG. 8. The radial size R_x of a condensate with a vortex in a prolate trap (γ=0.2). Solid curve: both s-wave and dipolar interactions. Dashed curve: s-wave only.

IV. AN EXPLICIT EXPRESSION FOR Ω_c

The effect that Ω_c is decreased in an oblate trap and increased in a prolate trap is the main result of this paper. Let us see if we can interpret this physically. The value of Ω_c shown in Figs. 6 and 11 for the purely s-wave interactions (dashed curve) agrees very well with the analytic formula valid in the Thomas-Fermi limit [14]

$$\Omega_c = \frac{5}{2}\frac{\hbar}{mR_x^2}\ln\frac{0.67R_x}{\xi_s}. \tag{30}$$

This is derived by integrating the kinetic energy density $n(\rho,z)v_s^2(\rho)/2$, arising from the superfluid flow

$$v_s = \frac{\hbar}{m\rho}$$

around the vortex, over the profile of the condensate. The lower limit of the integral is set by the vortex core size which is given by the healing length ξ_s

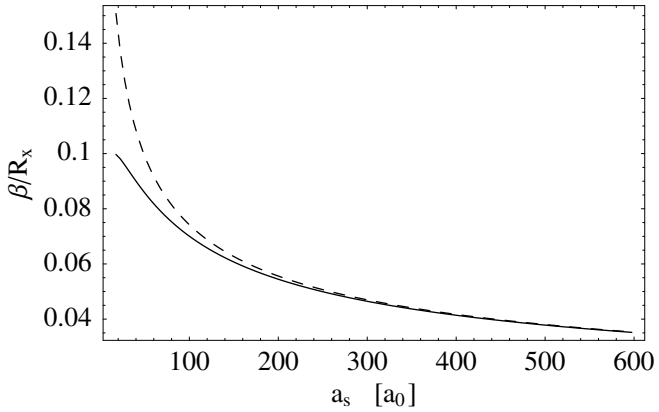

FIG. 9. The ratio of the vortex core size β to the radial size R_x of a condensate in a prolate trap (γ=0.2). Solid curve: both s-wave and dipolar interactions. Dashed curve: s-wave only.

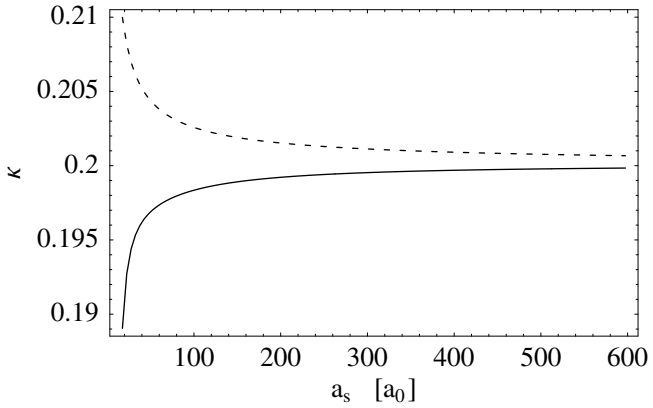

FIG. 10. The aspect ratio κ of a condensate with a vortex in a prolate trap (γ=0.2). Solid curve: both s-wave and dipolar interactions. Dashed curve: s-wave only.

$$\xi_s = \frac{1}{\sqrt{8\pi n_0 a_s}}. \tag{31}$$

The relevant density appearing in this expression is taken to be the density at the center of the trap n_0 in the absence of a vortex, which in the Thomas-Fermi limit is given by

$$n_0 = \frac{15N}{8\pi}\frac{1}{R_z R_x^2}. \tag{32}$$

In the Thomas-Fermi regime the radii of a condensate with s-wave interactions obey [2]

$$R_i = \bar{a}_{ho}\left(\frac{15Na_s}{\bar{a}_{ho}}\right)^{1/5}\frac{\bar{\omega}_{ho}}{\omega_i}, \tag{33}$$

where $\bar{\omega}_{ho}=(\omega_x\omega_y\omega_z)^{1/3}$ and $\bar{a}_{ho}=\sqrt{\hbar/(m\bar{\omega}_{ho})}$. Combining all these quantities together one finds that as $a_s\to 0$ the critical rotation frequency diverges as $\Omega_c \propto a_s^{-2/5}\log a_s$, although, of course, eventually the neglected quantum pressure term will prevent this divergence.

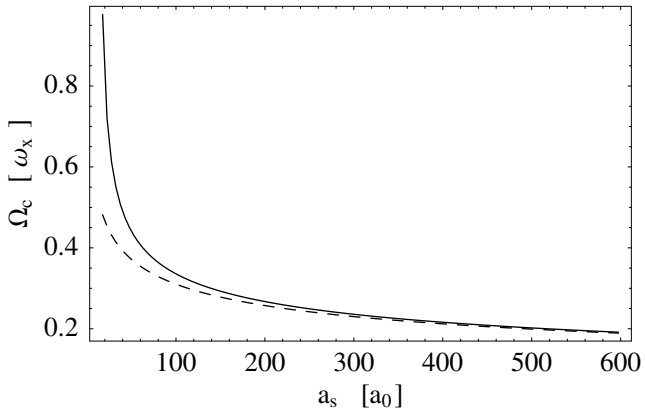

FIG. 11. The critical angular velocity Ω_c above which a vortex state is energetically favorable in a prolate trap (γ=0.2). Solid curve: both s-wave and dipolar interactions. Dashed curve: s-wave only.

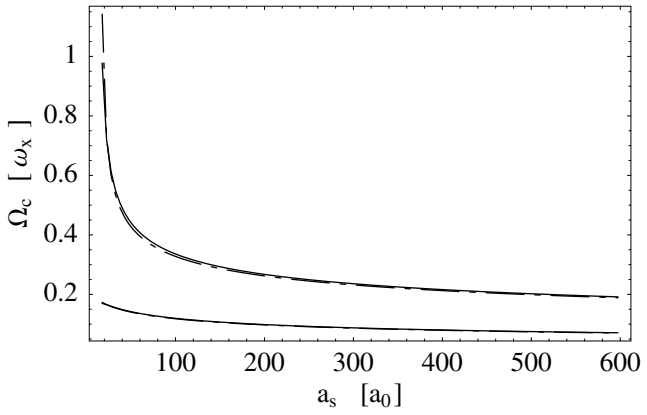

FIG. 12. Comparison of the critical angular velocity Ω_c calculated by the methods of Sec. III (solid curves) with the prediction of the analytic formula Eq. (30) where the condensate radius R_x is calculated for a dipolar BEC in the Thomas-Fermi limit with no vortex (dash-dot curves), see text for details. The upper two curves are for the prolate case, $\gamma=0.2$, and the lower two curves are for the oblate case, $\gamma=5$, as before. Note that the match is so good that it is hard to discern the difference between the solid and the dash-dot curves, except for very small a_s in the prolate case.

Now consider the dipolar case. A formula for Ω_c closely resembling Eq. (30) should still apply. Indeed, the inverted-parabola Thomas-Fermi density profile is common to both the *s*-wave and dipolar cases and it is this that gives rise to the specific 5/2 and 0.67 numerical factors appearing in Eq. (30). The one difference we might expect concerns the lower limit of the integration which is set by the vortex core size. In the presence of dipolar interactions we can no longer assert that the core size is solely determined by ξ_s since this makes no reference to dipolar interactions. Indeed, we might expect that as the scattering length vanishes it is replaced by an equivalent length scale set by the dipolar interactions of the form $a_d \equiv (C_{\rm dd}/3)m/(4\pi\hbar^2)$. However, expression (30) only has logarithmic accuracy [33] and is relatively insensitive to the lower cutoff ξ_s of the kinetic energy integral appearing inside the logarithm. The dominant change in Eq. (30) due to the presence of dipolar interactions is therefore likely to be in the radial size R_x. This makes one wonder whether the same expression (30) for Ω_c approximately holds for dipolar BECs if the radius R_x is modified to include the effect of the dipole-dipole interactions but the changes in the healing length are ignored? The answer to this question is yes [34] as we shall now show.

The Thomas-Fermi radii of a vortex-free BEC cylindrically symmetric in the *x*-*y* plane (dipoles aligned along *z*) with both contact and dipolar interactions are [25,26]

$$R_x = R_y = \left[\frac{15gN\kappa}{4\pi m\omega_x^2} \left\{ 1 + \varepsilon_{\rm dd} \left(\frac{3}{2} \frac{\kappa^2 f(\kappa)}{1-\kappa^2} - 1 \right) \right\} \right]^{1/5} \quad (34)$$

and $R_z = R_x/\kappa$. The function $f(\kappa)$ appearing in this expression is given by Eq. (18) and the value of κ is determined by the transcendental Eq. (22). In Fig. 12 we compare the value of Ω_c calculated by the energy minimization method presented in Sec. III with the value of Ω_c obtained from the explicit expression (30) where R_x is given by Eq. (34). The agreement is strikingly good, with the exception of very small a_s in the prolate case. In fact, in view of the closeness of the match one is tempted to conclude that while the long-range dipolar interactions strongly influence the boundary of the condensate and hence the large scales represented by R_x, the shorter range van der Waals interactions which set the scale for a_s and hence ξ_s continue to dominate the shorter range physics setting the size of the vortex core, except when a_s becomes very small indeed.

V. COMPARISON OF VORTICES WITH OTHER TYPES OF ANGULAR MOTION

We have seen in previous sections that for a dipolar BEC in a rotating prolate trap the formation of a vortex is increasingly energetically suppressed as the dipolar interactions grow in strength. Indeed, once $\Omega_c \geqslant \omega_x$ the vortex would be impossible to realize, in a harmonic trap at least, because the trap can no longer counteract the centrifugal force and the BEC would fly apart (neglecting, of course, the intriguing possibility that the attractive nature of the mean-field interactions might be capable of holding the condensate together for rotational frequencies Ω greater than ω_x). The question then arises, how does a prolate dipolar BEC rotate? One possibility is for the condensate to generate other types of excitation that can carry angular momentum such as quadrupole shape oscillations which have an azimuthal angular momentum projection $m=2$. In the frame of reference rotating with the trap a quadrupole oscillation appears as a stationary distortion of the density profile in the *x*-*y* plane [35,36] and it is generated through a bifurcation that has a threshold frequency Ω_b that in the pure *s*-wave case is typically considerably higher than Ω_c (in the case of an axisymmetric trap $\Omega_b = \omega_x/\sqrt{2}$). Dynamical instabilities of these shape oscillations play an important role in the *dynamics* of how a vortex actually enters the condensate, a subject we have not touched upon since we have only considered the energetics rather than the dynamics of vortex formation. In the case of pure *s*-wave condensates it is an experimental fact [17] that in order to generate vortices the trap must be rotated at a frequency considerably exceeding the condition of energetic stability given by Eq. (30) and instead corresponding closely to Ω_b.

The dynamical instability of a rotating dipolar BEC to shape oscillations has recently been investigated [37], and it was found that dipolar interactions always lower the threshold rotational frequency at which the instability occurs, in both the prolate *and* oblate cases. It is interesting to note that in the pure *s*-wave case the threshold frequency for the instability is *independent* of interaction strength (even though the instability relies on the existence of two-body interactions [2]) but, conversely, in the dipolar case is strongly affected by the magnitude of the interactions (but perhaps, based on the discussion of Sec. IV; the effect of dipolar interactions is simply through the degree to which these change the shape and aspect ratio of the condensate). One might tentatively conjecture, therefore, that as the critical rotation frequency for energetic favorability of the vortex

state goes up, and the critical rotation frequency for the dynamical instability goes down, shape oscillations will be formed that will not go on to form vortices.

Let us now also briefly consider another possibility, namely oscillations of the center of mass (c.m.). In a harmonic trap c.m. oscillations decouple from internal excitations provided the interactions are pairwise, and therefore take place at the trap frequency. Like low-lying shape oscillations, c.m. oscillations also preserve the parabolic density profile and so might be energetically preferable to a vortex in the presence of attractive interactions. Consider a BEC executing a c.m. oscillation of the form

$$\mathbf{r}_{cm}(t) = r_0 \cos(\omega_x t)\hat{\mathbf{x}} + r_0 \sin(\omega_x t)\hat{\mathbf{y}}, \tag{35}$$

where $\mathbf{r}_{cm}(t)$ is the position of center of mass of the BEC, which behaves like a classical particle of mass Nm with potential energy $NM\omega_x^2 r_{cm}^2/2$. This circular motion has an angular momentum $L_{cm}=Nm\omega_x r_0^2$, with the actual value of L_{cm} being determined by the radius r_0. Note that Eq. (35) describes dynamics obeying the superfluid irrotationality condition ($\nabla \times v_s = 0$) as may be verified by observing that the wave function which is an exact solution of the time-dependent Gross-Pitaevskii equation describing this type of motion is of the form [2]

$$\begin{aligned}\Psi(\mathbf{r},t) = &\exp[-i\mu t/\hbar]\exp\{i\alpha(t)[x - A(t)/2]/\hbar\} \\ &\times \exp\{i\beta(t)[y - B(t)/2]/\hbar\} \\ &\times \Psi_0[x - A(t), y - B(t), z],\end{aligned} \tag{36}$$

where $\Psi_0(x,y,z)$ is a stationary state satisfying the time-independent Gross-Pitaevskii equation, and the parameters $\{A(t),\alpha(t);B(t),\beta(t)\}$ obey $\alpha = m\dot{A}$, $Am\omega_x^2 = -\dot{\alpha}$ and $\beta = m\dot{B}$, $Bm\omega_x^2 = -\dot{\beta}$.

The energy associated with the type of c.m. oscillations given by Eq. (35) is $E_{cm}=Nm\omega_x^2 r_0^2$. In order to make a comparison between the energy of the vortex state and the c.m. motion we set $L_{cm}=N\hbar$, so that the two have the same angular momentum. Then $r_0^2=\hbar/(m\omega_x)$, i.e., the radius of motion is equal to the trap oscillator length, and so $E_{cm}^{L=N\hbar}=N\hbar\omega_x$. Noting that the ground state energy, E_0, is the same for both the vortex and c.m. motion, we can therefore compare E_{cm} with $E_v=N\hbar\Omega_c$. In order to be competitive with a vortex, c.m. motion with $L_{cm}=N\hbar$ would therefore require $\Omega_c \geqslant \omega_c$, but this is exactly the rotational speeds for which the harmonic trap no longer confines the atoms and so we surmise that c.m. motion is not energetically favorable over a vortex state in a harmonic trap. This does not preclude, however, that center of mass motion takes place in preference to other types of motion for angular momenta $L < N\hbar$. Also, perhaps center of mass motion can be favored in nonharmonic traps [38]

VI. CONCLUSIONS

The question of how quantum fluids rotate is a fascinating one. The versatility of atomic BECs means that this problem can now be studied in systems with repulsive or attractive interactions, as well as the case of dipole-dipole interactions which are partially repulsive, partially attractive, and of long range. In this paper we have used an approach based on an analogy to electrostatics that allows the explicit calculation of the anisotropic mean-field potential inside a dipolar BEC. This approach gives quite general insight and in particular shows that the long-range part of the interaction is especially important in places where the density profile has a large curvature in the direction of polarization, such as the ends of vortices. Numerical minimization of the total energy functional calculated by this method in the Thomas-Fermi regime indicates that, in comparison to the case of pure s-wave contact interactions, dipolar interactions lower the critical rotation frequency Ω_c of a BEC necessary to make a vortex energetically favorable in an oblate trap and raise the critical rotation frequency in a prolate trap. The same results can also be accurately reproduced using the analytic formula Eq. (30) well-known in the usual case of s-wave contact interactions providing the modification of the radius R_x of the BEC due to dipolar interactions is accounted for using Eq. (34). The analytic formula allows one to attribute the principal change in Ω_c caused by the dipolar interactions to changes in R_x, i.e., large-scale changes in the overall shape of the condensate, rather than changes on the much smaller scale of the healing length which determines the size of the vortex core. Finally, we have also discussed angular momentum carrying shape oscillations as well as center of mass oscillations as competitors to vortices in rotating prolate dipolar BECs, and tentatively conclude that under certain circumstances shape oscillations such as the quadrupole oscillation may be preferred.

ACKNOWLEDGMENTS

We would like to thank S. Giovanazzi and A.M. Martin for many discussions. We are indebted to J.M.F. Gunn for first suggesting to us the problem discussed in this paper and to L. Santos for proposing we try the explicit solution described in Sec. IV. We gratefully acknowledge financial support from the Engineering and Physical Sciences Research Council (EPSRC) of the UK as well as QIP-IRC postdoctoral funding (D.O'D)and from the Royal Society (C.E.).

APPENDIX: THE ENERGY FUNCTIONALS

In this appendix we write down the explicit expressions for the functionals giving the kinetic, trapping, s-wave scattering, and dipolar interaction energy of the condensate, as defined by Eqs. (7), (8), (10), and (11), respectively. Beginning with the kinetic energy, we first note that in cylindrical coordinates the gradient is given by

$$\nabla = \hat{\mathbf{e}}_\rho \frac{\partial}{\partial \rho} + \hat{\mathbf{e}}_\phi \frac{1}{\rho}\frac{\partial}{\partial \phi} + \hat{\mathbf{e}}_z \frac{\partial}{\partial z}, \tag{A1}$$

which acts upon the wave function given by the square root of the density ansatz (24)

$$\Psi(\rho,\phi,z) = \sqrt{n_0}\sqrt{1-\frac{\rho^2}{R_x^2}-\frac{z^2}{R_z^2}}\sqrt{1-\frac{\beta^2}{\rho^2+\beta^2}}e^{i\phi}. \tag{A2}$$

The phase ϕ accounts for the superflow around the vortex in the usual way, viz. $\mathbf{v}_s=(\hbar/m)\nabla\phi$ [2]. However, the Thomas-Fermi approximation corresponds to neglecting the kinetic energy arising from the curvature of the slowly varying condensate background envelope $\sqrt{1-\rho^2/R_x^2-z^2/R_z^2}$. We shall consequently drop all terms which originate from the gradient of this term. On the other hand, it is essential to retain the terms arising from the gradient of the vortex part of the wave function $\sqrt{1-\beta^2/(\rho^2+\beta^2)}$ which varies rapidly in the $\hat{\mathbf{e}}_\rho$ direction, as well as the superflow term. Under these approximations we find the kinetic energy to be

$$E_{\text{kinetic}} = \frac{\hbar^2}{2m}\frac{n_0\pi R_z}{3}\left\{-11\bar{\beta}^2-\frac{26}{3} + \frac{11\bar{\beta}^4+16\bar{\beta}^2+8}{\sqrt{1+\bar{\beta}^2}}\operatorname{arctanh}[1/\sqrt{1+\bar{\beta}^2}]\right\}, \tag{A3}$$

where n_0 is the number density at the center of the trap, as given by Eq. (27).

Using the density ansatz (24) the trapping and s-wave scattering energies are straightforwardly evaluated to be

$$E_{\text{trap}} = \frac{2\pi}{3}n_0 m\omega_x^2\frac{R_x^5}{\kappa}\left\{\frac{4}{35}-\frac{2}{5}\bar{\beta}^2-\frac{8}{3}\bar{\beta}^4-2\bar{\beta}^6 + \frac{2\gamma^2}{5\kappa^2}\left(\frac{1}{7}+\frac{23}{15}\bar{\beta}^2+\frac{7}{3}\bar{\beta}^4+\bar{\beta}^6\right) + 2\bar{\beta}^2\left[\bar{\beta}^2-\frac{\gamma^2}{5\kappa^2}(1+\bar{\beta}^2)\right](1+\bar{\beta}^2)^{3/2} \times\operatorname{arctanh}(1/\sqrt{1+\bar{\beta}^2})\right\} \tag{A4}$$

and

$$E_{\text{sw}} = \frac{8\pi}{15}gn_0^2\frac{R_x^3}{\kappa} \times\left[\frac{2}{7}+\frac{107}{15}\bar{\beta}^2+16\bar{\beta}^4+9\bar{\beta}^6-\bar{\beta}^2(4+13\bar{\beta}^2 + 9\bar{\beta}^4)\sqrt{1+\bar{\beta}^2}\times\operatorname{arctanh}(1/\sqrt{1+\bar{\beta}^2})\right]. \tag{A5}$$

The dipolar energy functional is more difficult to calculate since the dipolar mean-field potential $\Phi_{\text{dd}}(\mathbf{r})$ is nonlocal. In the text we argued that

$$E_{\text{dd}} \approx \frac{1}{2}\int d^3r\, n_{\text{bg}}(\mathbf{r})\Phi_{\text{dd}}^{\text{bg}}(\mathbf{r}) + \int d^3r n_{\text{v}}(\mathbf{r})\Phi_{\text{dd}}^{\text{bg}}(\mathbf{r}), \tag{A6}$$

where $\Phi_{\text{dd}}^{\text{bg}}(\mathbf{r})$ is given by the quadratic function Eq. (17). These two integrals can be evaluated explicitly and the results are

$$\frac{1}{2}\int d^3r\, n_{\text{bg}}(\mathbf{r})\Phi_{\text{dd}}^{\text{bg}}(\mathbf{r}) = -\frac{16\pi g n_0^2}{105\kappa}\varepsilon_{\text{dd}}R_x^3 f(\kappa) \tag{A7}$$

and

$$\int d^3r\, n_{\text{v}}(\mathbf{r})\Phi_{\text{dd}}^{\text{bg}}(\mathbf{r}) = -\frac{4\pi}{15}n_0^2 g\varepsilon_{\text{dd}}\frac{R_x^3}{\kappa}\bar{\beta}^2\left\{\frac{122}{15}+\frac{68}{3}\bar{\beta}^2+14\bar{\beta}^4+\frac{f(\kappa)}{15(\kappa^2-1)} \times[-62+245\kappa^2+30\bar{\beta}^2(2+15\kappa^2)+45\bar{\beta}^4(2+5\kappa^2)] - (1+\bar{\beta}^2)^{3/2}\operatorname{arctanh}(1/\sqrt{1+\bar{\beta}^2})\left[4+14\bar{\beta}^2+\frac{f(\kappa)}{\kappa^2-1} \times(-4+10\kappa^2+6\bar{\beta}^2+15\kappa^2\bar{\beta}^2)\right]\right\}. \tag{A8}$$

[1] A. Griesmaier, J. Werner, S. Hensler, J. Stuhler, and T. Pfau, Phys. Rev. Lett. **94**, 160401 (2005).
[2] L. Pitaevskii and S. Stringari, *Bose-Einstein Condensation* (Oxford, New York, 2003).
[3] J. Werner, A. Griesmaier, S. Hensler, J. Stuhler, T. Pfau, A. Simoni, and E. Tiesinga, Phys. Rev. Lett. **94**, 183201 (2005).
[4] L. Santos, G. V. Shlyapnikov, P. Zoller, and M. Lewenstein, Phys. Rev. Lett. **85**, 1791 (2000).
[5] S. Yi and L. You, Phys. Rev. A **63**, 053607 (2001).
[6] K. Góral, K. Rzążewski, and T. Pfau, Phys. Rev. A **61**, 051601(R) (2000); J.-P. Martikainen, M. Mackie, and K.-A. Suominen, *ibid.* **64**, 037601 (2001).
[7] K. Góral and L. Santos, Phys. Rev. A **66**, 023613 (2002).
[8] P. M. Lushnikov, Phys. Rev. A **66**, 051601(R) (2002).
[9] L. Santos, G. V. Shlyapnikov, and M. Lewenstein, Phys. Rev. Lett. **90**, 250403 (2003).
[10] D. H. J. O'Dell, S. Giovanazzi, and G. Kurizki, Phys. Rev. Lett. **90**, 110402 (2003).
[11] L. P. Pitaevskii, Zh. Eksp. Teor. Fiz. **39**, 423 (1984) , [JETP Lett. **39**, 511 (1984)].
[12] S. Giovanazzi and D. O'Dell, Eur. Phys. J. D **31**, 439 (2004).
[13] F. Dalfovo and S. Stringari, Phys. Rev. A **53**, 2477 (1996).
[14] E. Lundh, C. J. Pethick, and H. Smith, Phys. Rev. A **55**, 2126 (1997).
[15] D. L. Feder, C. W. Clark, and B. I. Schneider, Phys. Rev. Lett. **82**, 4956 (1999).
[16] M. R. Matthews, B. P. Anderson, P. C. Haljan, D. S. Hall, C. E. Wieman, and E. A. Cornell, Phys. Rev. Lett. **83**, 2498 (1999).
[17] K. W. Madison, F. Chevy, W. Wohlleben, and J. Dalibard, Phys. Rev. Lett. **84**, 806 (2000); K. W. Madison, F. Chevy, V. Bretin, and J. Dalibard, *ibid.* **86**, 4443 (2001).
[18] C. Raman, J. R. Abo-Shaeer, J. M. Vogels, K. Xu, and W.

Ketterle, Phys. Rev. Lett. **87**, 210402 (2001).
[19] N. K. Wilkin, J. M. F. Gunn, and R. A. Smith, Phys. Rev. Lett. **80**, 2265 (1998).
[20] J. M. F. Gunn (private communication).
[21] C. J. Pethick and H. Smith, *Bose-Einstein Condensation in Dilute Gases* (Cambridge University, Cambridge, England, 2002), see, in particular, Fig. 9.3.
[22] L. D. Carr and C. W. Clark, Phys. Rev. Lett. **97**, 010403 (2006).
[23] J. Stuhler, A. Griesmaier, T. Koch, M. Fattori, T. Pfau, S. Giovanazzi, P. Pedri, and L. Santos, Phys. Rev. Lett. **95**, 150406 (2005).
[24] S. Giovanazzi, A. Görlitz, and T. Pfau, J. Opt. B: Quantum Semiclassical Opt. **5**, S208 (2003).
[25] D. H. J. O'Dell, S. Giovanazzi, and C. Eberlein, Phys. Rev. Lett. **92**, 250401 (2004).
[26] C. Eberlein, S. Giovanazzi, and D. H. J. O'Dell, Phys. Rev. A **71**, 033618 (2005).
[27] N. R. Cooper, E. H. Rezayi, and S. H. Simon, Phys. Rev. Lett. **95**, 200402 (2005).
[28] J. Zhang and H. Zhai, Phys. Rev. Lett. **95**, 200403 (2005).
[29] S. Yi and H. Pu, Phys. Rev. A **73**, 061602(R) (2006).
[30] This is most easily seen by comparing the Fourier transform of the dipolar interaction (1), i.e., $\tilde{U}_{\mathrm{dd}}(\mathbf{k})=\Sigma_{i,j}\frac{C_{\mathrm{dd}}}{3}\hat{e}_i\hat{e}_j(3\hat{k}_i\hat{k}_j-\delta_{ij})$, with that of the contact interaction, i.e., $\tilde{U}(\mathbf{k})=g$. One immediately sees that $\varepsilon_{\mathrm{dd}}=1$ corresponds to the case when the isotropic term in the dipole-dipole interaction is exactly equal and opposite to the contact interaction.
[31] M. Marinescu and L. You, Phys. Rev. Lett. **81**, 4596 (1998).
[32] S. Giovanazzi, A. Görlitz, and T. Pfau, Phys. Rev. Lett. **89**, 130401 (2002).
[33] E. M. Lifshitz and L. P. Pitaevskii, *Statistical Physics Part 2* (Butterworth-Heinemann, Oxford, 1998).
[34] L. Santos (private communication).
[35] A. Recati, F. Zambelli, and S. Stringari, Phys. Rev. Lett. **86**, 377 (2001).
[36] S. Sinha and Y. Castin, Phys. Rev. Lett. **87**, 190402 (2001).
[37] R. M. W. van Bijnen, D. H. J. O'Dell, N. G. Parker, and A. M. Martin, e-print cond-mat/0602572.
[38] A. Lundh, A. Collin, and K. -A. Suominen, Phys. Rev. Lett. **92**, 070401 (2004).